

DISCLAIMER

This report was prepared as an account of work sponsored by an agency of the United States Government. Neither the United States Government nor any agency thereof, nor any of their employees, makes any warranty, express or implied, or assumes any legal liability or responsibility for the accuracy, completeness, or usefulness of any information, apparatus, product, or process disclosed, or represents that its use would not infringe privately owned rights. Reference herein to any specific commercial product, process, or service by trade name, trademark, manufacturer, or otherwise does not necessarily constitute or imply its endorsement, recommendation, or favoring by the United States Government or any agency thereof. The views and opinions of authors expressed herein do not necessarily state or reflect those of the United States Government or any agency thereof. Reference herein to any social initiative (including but not limited to Diversity, Equity, and Inclusion (DEI); Community Benefits Plans (CBP); Justice 40; etc.) is made by the Author independent of any current requirement by the United States Government and does not constitute or imply endorsement, recommendation, or support by the United States Government or any agency thereof.

PNNL-38798

Passive Acoustic Monitoring of a Riverine Turbine with Stationary Hydrophones

December, 2025

Emma Cotter

Joseph Haxel

James McVey

DISCLAIMER

This report was prepared as an account of work sponsored by an agency of the United States Government. Neither the United States Government nor any agency thereof, nor Battelle Memorial Institute, nor any of their employees, makes **any warranty, express or implied, or assumes any legal liability or responsibility for the accuracy, completeness, or usefulness of any information, apparatus, product, or process disclosed, or represents that its use would not infringe privately owned rights.** Reference herein to any specific commercial product, process, or service by trade name, trademark, manufacturer, or otherwise does not necessarily constitute or imply its endorsement, recommendation, or favoring by the United States Government or any agency thereof, or Battelle Memorial Institute. The views and opinions of authors expressed herein do not necessarily state or reflect those of the United States Government or any agency thereof.

PACIFIC NORTHWEST NATIONAL LABORATORY
operated by
BATTELLE
for the
UNITED STATES DEPARTMENT OF ENERGY
under Contract DE-AC05-76RL01830

Printed in the United States of America

Available to DOE and DOE contractors from
the Office of Scientific and Technical Information,
P.O. Box 62, Oak Ridge, TN 37831-0062
www.osti.gov
ph: (865) 576-8401
fox: (865) 576-5728
email: reports@osti.gov

Available to the public from the National Technical Information Service
5301 Shawnee Rd., Alexandria, VA 22312
ph: (800) 553-NTIS (6847)
or (703) 605-6000
email: info@ntis.gov
Online ordering: <http://www.ntis.gov>

Passive Acoustic Monitoring of a Riverine Turbine with Stationary Hydrophones

December, 2025

Emma Cotter
James McVey

Joseph Haxel

Prepared for
the U.S. Department of Energy
Under Contract DE-AC05-76RL01830

Pacific Northwest National Laboratory
Richland, Washington 99352

Acknowledgments

The authors wish to thank the Igiugig Village Council and members of the Igiugig Village for their support with planning, vessel operations, and hospitality. We also thank the Ocean Renewable Power Company (ORPC) for supporting turbine operation, Brian Polagye and Christopher Bassett at the University of Washington for helpful conversations on interpretation of results, Christopher Rumple and Linnea Weicht at PNNL for support preparing equipment for deployment, Garrett Staines at PNNL for support with logistics and planning, and Samantha Eaves and Denis-Marc Nault at the Department of Energy for guidance and feedback during planning.

Contents

Acknowledgments	iv
Abstract	vii
1.0 Introduction	1
2.0 Test Site	2
3.0 Interpreting the Technical Specification	4
4.0 Methods	6
4.1 Instrumentation	6
4.2 Data Collection	6
4.3 Data Processing	9
4.4 Frequency Limits	10
5.0 Results	13
6.0 Discussion & Conclusions	17
Appendix A Sound Speed Profile	A.1
Appendix B Hydrophone Location Comparison	B.1
Appendix C Weighted Cumulative Sound Exposure Level	C.1

Figures

1	Map showing bathymetry of the area of the Kvichak river where the turbines are deployed. The locations of the two turbines (RG1 and RG2) are indicated, and the white box indicates the area shown in Figure 3. Bathymetry data are from Terrasond 2015.	3
2	Hydrophone lander prior to deployment with weights on the foot of each tripod leg. The icListen HF SC2 hydrophone, equipped with a flow shield, is shown.	6
3	Map indicating four hydrophone locations and the approximate centers of both turbines in the Kvichak River. RG1 can be seen underwater in the satellite image, but RG2 (not operational during this study) was deployed after this image was taken.	7
4	Approximate modal cut-off frequency, calculated using Equation 5, for various values of the speed of sound in the riverbed (c_s) and depth at the hydrophone (D)	11
5	Median decidecade sound pressure spectral density levels recorded during each turbine operational state at H1 (a.), H2 (b.), H3 (c.), and H4 (d.). The shaded region indicates the interquartile range.	14
6	Median mean-squared pressure level recorded during each turbine operational state at H1 (a.), H2 (b.), H3 (c.), and H4 (d.). The shaded region indicates the interquartile range.	14
7	Probability from a two-sided Kolmogorov-Smirnov test comparing decidecade sound pressure levels ($L_{p,ddec}$) measured during 100% power generation and braked operations at sites H1 (a.), H2 (b.), H3 (c.), and H4 (d.). The red dashed line depicts a P-value of 0.05, and the red shaded region covers frequency bands that have a P-value greater than 0.05, meaning the compared distributions most likely do not come from the same distribution.	15
A.1	Sound speed profile measured on 28 May, 2024.	A.1
B.2	Median decidecade sound pressure levels recorded at each hydrophone location when the turbine was operated in freewheel (a.), at 25% (b.), 50% (c.), 75% (d.), and 100% power (e.), and when the turbine was braked (f.). The shaded region indicates the interquartile range.	B.1
B.3	Median mean-squared pressure spectral density level recorded at each hydrophone location when the turbine was operated in freewheel (a.), at 25% (b.), 50% (c.), 75% (d.), and 100% power (e.), and when the turbine was braked (f.). The shaded region indicates the interquartile range.	B.2

Abstract

In this study, we characterize the sound generated by a cross-flow riverine turbine in the Kvichak River near Igiugig, Alaska, United States. To do this, we follow the International Electro-technical Commission (IEC) technical specification for characterization of the acoustic emissions from marine energy converters. While marine mammals do not inhabit the test site, the U.S. National Marine Fisheries Service (NMFS) guidelines for assessing the effects of anthropogenic sound on marine mammal hearing were implemented to provide context for the deployment of similar turbines in other areas. The results indicate that turbine sound at the measurement locations was not predicted to be harmful to marine mammals. Results also provide insight into the acoustic characteristics of current energy converters and the complex acoustic propagation in rivers.

1.0 Introduction

Marine energy converters, including wave, tidal, and riverine current energy converters, can provide a source of reliable renewable power for coastal communities or at-sea applications. However, responsible development and regulatory approval of these technologies requires an understanding of their effects on the environment. Sound generated by marine energy converters is one of several environmental stressors that drive permitting and acceptance of these new technologies (Garavelli et al. 2024). Many aquatic animals, including marine mammals and fish, use underwater sound for communication, navigation, or foraging. Underwater sound from anthropogenic sources can affect animal behavior, habitat use, and, in extreme cases, cause injury or mortality (Rako-Gospic and Picciulin 2019). As such, it is highly regulated and uncertainty around the acoustic impacts of marine energy converters is often part of regulatory processes in the United States. Therefore, characterizing the radiated sound from marine energy converters can reduce barriers to testing and shorten regulatory timelines by providing reference points for scientists, regulators, and marine energy developers (Garavelli et al. 2024).

Measuring the radiated sound from marine energy converters is not straightforward given the presence of other anthropogenic and ambient noise, impacts of flow noise on acoustic recordings, and variations in radiated noise with device operating state. Therefore, a technical specification (62600-40) has been developed by the International Electrotechnical Commission TC 114 to facilitate characterization of the acoustic emissions from marine energy converters in a manner that is both robust and comparable to other measurements (International Electrotechnical Commission 2019). Acoustic characterization following the technical specification can utilize either drifting or stationary hydrophones. In this report, we detail the acoustic characterization of a riverine turbine deployed in the Kvichak River in Igiugig, Alaska (AK), United States using stationary hydrophones. First, we describe the test site and how the requirements of the technical specification were applied to this study. Then, we detail our methodology for data collection and data processing. Finally, we present our results and make recommendations for acoustic characterization of riverine current energy converters.

2.0 Test Site

Igiugig Village is a federally recognized Alaska Native entity located near the mouth of the Kvichak River where it flows out from Lake Iliamna. The Igiugig Village Council holds a pilot license (FERC docket number P-13511) to operate two in-river turbines to provide renewable power for the village; the turbines are manufactured and operated by the Ocean Renewable Power Company (ORPC). Figure 1 shows the bathymetry of the river and the locations of the two turbines. In the area where the turbines are deployed, the river is approximately 5 m deep and the riverbed is a mix of gravel and cobbles, with little sand or silt (Terrasond 2015). Peak flow speeds in the main channel of the river where the turbines are located are approximately 2.5 m/s. However, the upriver island and the shallow river bank result in lower flow speeds on the east side of the river. Similarly, while the bank is much steeper on river right, flow around the upriver island creates a back-eddy with relatively quiescent water (Terrasond 2015). Hydrophones were deployed in these areas of lower flow.

Each bottom-mounted helical cross-flow turbine has two rotors that are 5 m long with a diameter of 1.8 m. During the work described in this report, only the upriver turbine (RG1) was operational, and the downriver turbine (RG2) was braked during all passive acoustic measurements. A detailed performance characterization of RG1 can be found in Forbush et al. 2016.

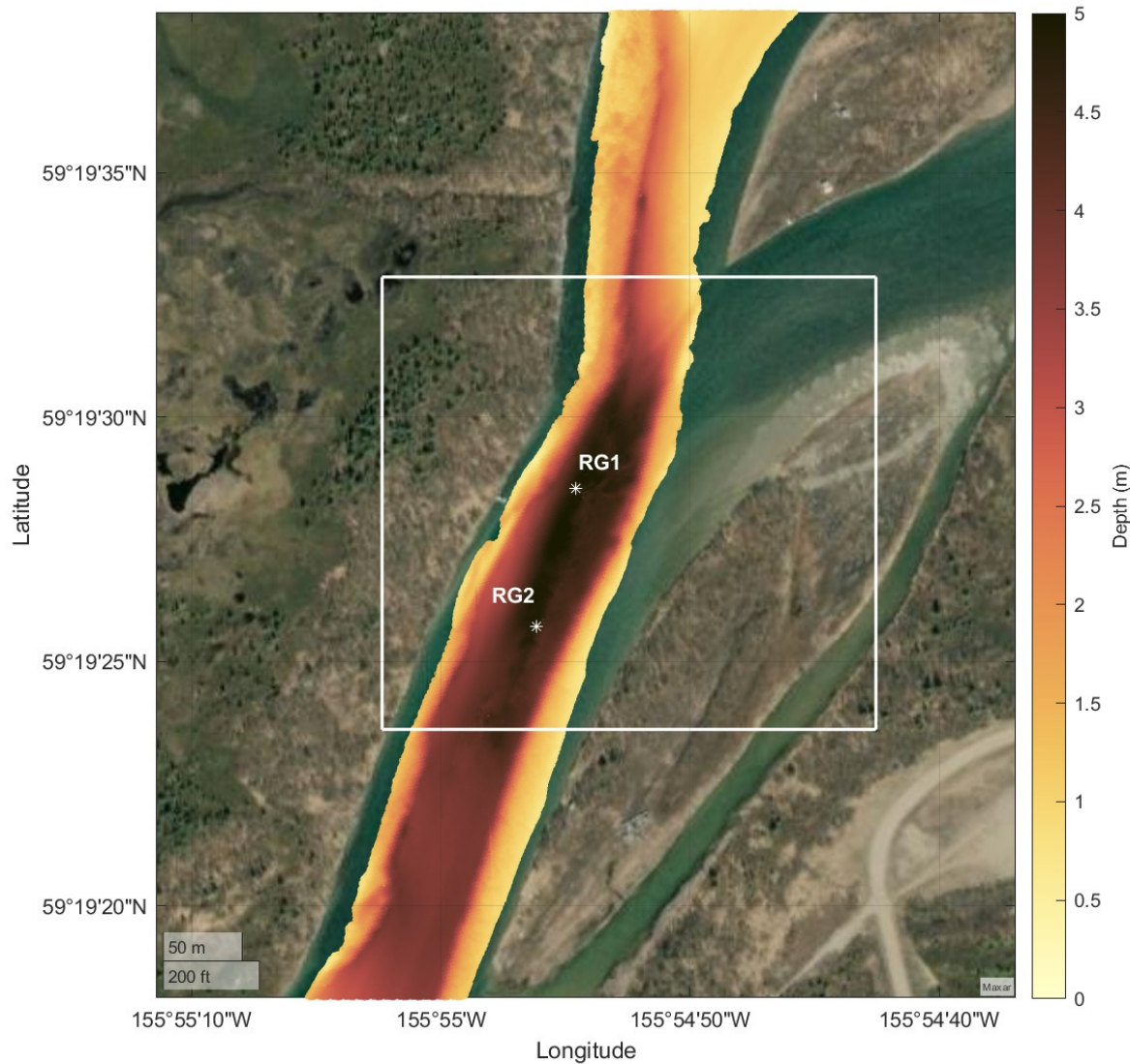


Figure 1. Map showing bathymetry of the area of the Kuchak river where the turbines are deployed. The locations of the two turbines (RG1 and RG2) are indicated, and the white box indicates the area shown in Figure 3. Bathymetry data are from Terrasond 2015.

3.0 Interpreting the Technical Specification

The IEC technical specification provides guidance for two levels of acoustic characterization: “Level A,” which offers spatially resolved acoustic measurements, and “Level B,” which has lower spatial and temporal resolution. Our study is closest to a “Level A” characterization, but has some differences from the methodology prescribed in the specification. Because the specification was primarily developed with wave and tidal energy converters in mind, some changes were required for implementation in a riverine environment. Further, the logistical constraints of working in a remote location required some adjustments to our methodology. Despite these changes in data collection methodology, all data were processed using the equations and metrics described in the specification. Table 1 provides a summary of the key data collection requirements for a Level A characterization of a current energy converter with fixed hydrophones described in the IEC 62600-40 technical specification and a discussion of how each requirement was interpreted or adjusted for this campaign.

We note that we chose to perform a characterization with stationary hydrophones because another research group was conducting a survey of the same turbine with drifting hydrophones. Comparison between results from the two methodologies will be included in a future publication.

Technical Specification Requirement	Application to this Study
<i>For fixed measurements, the pressure-sensitive element of the hydrophone shall be at least 1 m above the seabed, but no more than one-half of the water depth</i>	The shallow bathymetry of the hydrophone deployment locations (< 1.5 m) required hydrophones to be closer to the seabed (0.6 m elevation).
<i>Measurements should be made within four 25 m square “zones” located 100 m upstream, downstream, port, and starboard of the turbine.</i>	Hydrophone deployment locations were limited by strong currents, available vessels, and the width of the river. Hydrophone locations are detailed in Section 4.2.
<i>Measurements should be reported between 10 Hz and 100 kHz, meaning that the sample rate should be at least 256 kHz. The low frequency limit can be adjusted to account for the modal cutoff at the site based on depth and sound speed, and the high frequency limit can be adjusted based on the highest frequency of sound produced by the turbine.</i>	Hydrophones sampled at 256 kHz. The shallow location of the hydrophones on the riverbanks resulted in a modal cutoff frequency above 10 Hz, discussed in Section 4.4.
<i>Measurements should be conducted during currents that result in power output of 0%, 25%, 50%, 75%, and 100% of rated capacity.</i>	River current speeds did not change appreciably during the deployment, but the turbine power output was varied by ORPC.
<i>A water property or sound speed profile should be obtained within one hour of each hydrophone deployment.</i>	A sound speed profile was taken after hydrophone recovery.
<i>If a flow shield has been used to reduce flow noise, the effect of the flow shield on propagating sound and sound measurement system self-noise should be quantified.</i>	The flow shields used were characterized in Cotter et al. 2024.
<i>For fixed hydrophone measurements, neither a qualitative nor a quantitative assessment of wind speed is required.</i>	Quantitative wind speed measurements were recorded to assess any changes in ambient noise levels due to the proximity of the hydrophones to the water surface.
<i>An acoustic measurement sequence is a 1 s window of continuous samples converted to the frequency domain. For each spatial bin and turbine power rating, 10 valid samples are required.</i>	Because stationary hydrophones were deployed for multiple days, more than 10 samples were collected for each turbine power rating (Table 3).
<i>The complete sound measurement system should be calibrated immediately before and after the measurement session at one or more frequencies. The hydrophone calibration over the specified frequency range should be updated every 24 months.</i>	Hydrophone calibration immediately before and after measurement was not feasible due to time and funding constraints, but all hydrophones were calibrated. Details are provided in Section 4.2.

Table 1. Requirements of the IEC TS 62600-40 technical standard for a Level A acoustic characterization of a current energy converters and how they were applied or adjusted in this study.



Figure 2. Hydrophone lander prior to deployment with weights on the foot of each tripod leg. The icListen HF SC2 hydrophone, equipped with a flow shield, is shown.

4.0 Methods

4.1 Instrumentation

Sound pressure measurements were made with three Ocean Sonics icListen HF hydrophones equipped with oil-filled flow shields (Cotter et al. 2024). Each hydrophone was a different model of icListen hydrophone: one SJ9, one RB9, and one SC2. The only functional difference between the three models is the hydrophone element, which has been changed in different versions of the sensor. All three hydrophones were configured to sample at 256 kHz, resulting in a measured acoustic frequency range from 10-100 kHz. Hydrophones were deployed on gravity-anchored tripod landers (Figure 2) that positioned the omni-directional hydrophone sensors approximately 60 cm above the river bottom. The hydrophones were cabled to Ocean Sonics Launch Boxes on shore, which provided power and communication with the hydrophones for data quality control and archival. A SonTek CastAway profiling conductivity, temperature, and depth (CTD) sensor was used to measure sound speed in the river, and a Kestrel 1000 handheld anemometer was used to measure wind speed. No flow speed measurements were conducted, though acoustic Doppler current profiler (ADCP) measurements from the turbine platform were provided by ORPC.

Calibration of all three hydrophones was conducted at Ocean Networks Canada's HydroCal facility in 2025. Two separate calibrations were conducted; a very low frequency calibration that spanned 1 to 700 Hz and a high frequency calibration that spanned 2 to 130 kHz. The very low frequency calibration was conducted in 2023 for two of the hydrophones (RB9 and SC2), and less than 1 dB of variability between the years was observed.

4.2 Data Collection

Hydrophone data were collected on two separate days: 27 and 28 May, 2024. Hydrophone landers were deployed by a project team member wading into the river and lowering the tripod to the riverbed by hand at a depth of approximately 1.25 m. This approach was selected over deployment of hydrophones in the deeper water in the main channel of the river for two primary reasons. First, the lower flow speeds in the eddies along the river edge minimized flow noise

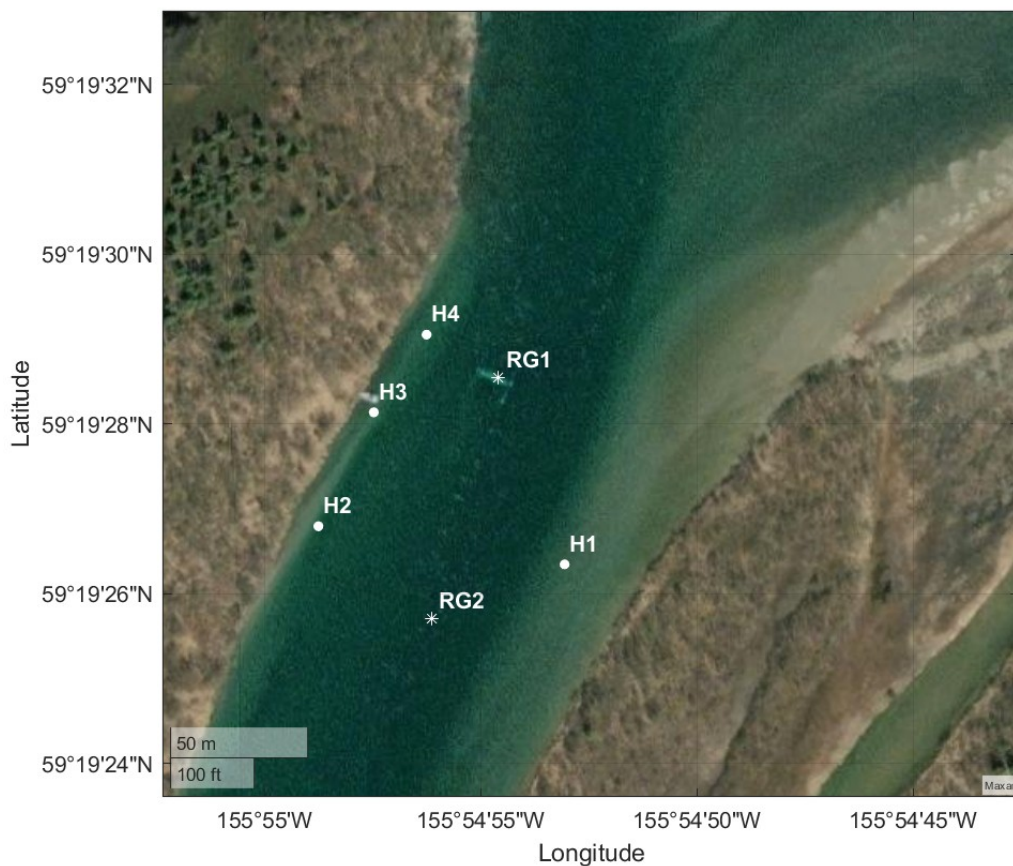


Figure 3. Map indicating four hydrophone locations and the approximate centers of both turbines in the Kovichak River. RG1 can be seen underwater in the satellite image, but RG2 (not operational during this study) was deployed after this image was taken.

Location	Longitude	Latitude	Distance from RG1 (m)
H1	155.914741° W	59.323985° N	72
H2	155.916322° W	59.324110° N	85
H3	155.915966° W	59.324483° N	47
H4	155.915627° W	59.324737° N	30

Table 2. Location of each hydrophone and its distance from the center of the operational turbine (RG1)

contamination. Second, deployment in the main channel of the river would have required a suitable vessel for deployment of an instrumentation platform with sufficient ballast to remain stationary in the stronger flows, which was not budgeted in this project. Further, had a vessel been available, sensor deployment in the main channel of the river would have been complex and risky in the strong currents. This stands in contrast with a tidal energy site, where instrumentation deployment operations can leverage periods of slack water during tidal exchanges.

Cables back to shore were weighted with sandbags to minimize any flutter noise induced by the currents. The location of each hydrophone was then recorded by a PNNL team member holding an Emlid Reach RS2 handheld GPS receiver over the lander. The three hydrophone landers were deployed at four distinct locations, shown in Figure 3. Table 2 lists the GPS coordinates of each hydrophone location and its distance from the center of the turbine. On 27 May, the SJ9, SC2, and RB9 hydrophones were deployed at locations H1, H3, and H4, respectively. On 28 May, the SJ9 hydrophone was moved to H2 and the SC2 and RB9 hydrophones remained at H3 and H4, respectively. These locations were all outside of the main channel of the river and experienced relatively low flow speeds, though a measurement of flow speed at each hydrophone location was not conducted.

Internal hydrophone clocks were synchronized to the clock of a single data collection computer at deployment. The data collection computer was synchronized to an internet time server prior to operations.

On each day of data collection, the operational turbine was cycled through various power states to assess any changes in the acoustic signature. On 27 May, approximately 30 minutes were recorded while the turbine was braked (0% power), at 100% power, 75% power, 50% power, 25% power, and freewheeling (i.e., rotating freely in the currents, but disconnected from the generator so as not to produce power), respectively. Power levels are relative to the maximum power output achievable during the sampling window based on flow speeds, and fluctuated during the recording period. On 28 May, approximately 20 minutes were recorded at each state. Wind speed was recorded from a point on the riverbank between H3 and H4 at least once every hour during hydrophone recording, and a log of passing vessels and airplanes was maintained to facilitate identification of non-turbine sound sources. A CTD cast was conducted after recovering hydrophones on 28 May in the thalweg of the river, downstream of the turbine.

We note that concurrent environmental monitoring efforts involved the use of 120 and 200 kHz echosounders for fish monitoring. While these operating frequencies are outside of the range measured by the hydrophones, active acoustic sensors can produce out-of-band sound at lower frequencies (Cotter et al. 2019). A shut-down test of these echosounders during hydrophone recording indicated that they did not contaminate passive acoustic measurements.

Date	Braked	Freewheel	25%	50%	75%	100%
27 May	370	135	170	115	170	75
28 May	160	95	90	75	24	30

Table 3. Number of high-quality one second samples identified through human review of spectrograms during each turbine operational state on each day of recording.

4.3 Data Processing

After all hydrophones were recovered, manual quality control of the recordings was conducted to ensure data quality and isolate periods of data for analysis. An analyst visually reviewed spectrograms to identify periods of data samples devoid of vessel traffic, airplanes, and other types of non-turbine operation related noise (e.g. nearby construction sounds, banging metal from a loose shackle). This also served to confirm times of non-turbine related noise contamination events observed by PNNL staff on site and recorded in the field notes. After manual screening, a total of 1180 seconds on 27 May and 494 seconds on 28 May of high quality data were isolated for further analysis and characterization of turbine related sounds (Table 3). As evidenced by the lower number of samples identified on 28 May, there were higher ambient noise levels on the second day of recording. Therefore, we limit our analysis of hydrophone locations H3 and H4, which had data from both days, to samples recorded on 27 May.

Data from the three hydrophones were aligned in time using the cross correlation between periods of data containing distinct acoustic signals (e.g., turbine startup or passing vessel). While each individual hydrophone was synchronized to a computer at the time of deployment, the lack of synchronization between the hydrophones during recording meant that there was some drift between their internal clocks. This lag was different on each day of recording due to hydrophone redeployment. Cross-correlation revealed that all three hydrophone clocks were within 2.1 and 1.5 s of each other on 27 and 28 May, respectively.

After aligning hydrophones in time and periods of data from each turbine operational state for analysis, data were processed following the IEC technical specification 62600-40. A brief overview of these calculations is provided here for reference. First, the voltage timeseries was separated into 1 s (256,000 samples) windows with 50% overlap, and each window was detrended and weighted using a Hann window. Then, the one-sided discrete Fourier transform (DFT) of each window was calculated using the fast Fourier transform (FFT), yielding the mean-squared voltage spectral density. The mean-squared voltage spectral density was adjusted so that the variance matched the voltage time series window before applying the frequency-dependent hydrophone sensitivity to convert to units of pressure, yielding the mean-squared pressure spectral density, $\overline{p_f^2}$, in $\mu\text{Pa}^2/\text{Hz}$. Results are reported in dB re 1 $\mu\text{Pa}^2/\text{Hz}$, or

$$L_{p,f} = 10 \log_{10} \frac{\overline{p_f^2}}{p_0^2} \quad (1)$$

where $L_{p,f}$ is the mean-squared pressure spectral density level and p_0^2 is the reference value of 1 $\mu\text{Pa}^2/\text{Hz}$. Decidecade sound pressure levels, $L_{p,ddec}$, in dB re 1 $\mu\text{Pa}^2/\text{Hz}$ were then calculated as

$$L_{p,ddec} = 10 \log_{10} \left(\frac{\int_{f_1}^{f_2} \overline{p_f^2} df}{p_0^2} \right), \quad (2)$$

where f_1 and f_2 are the upper and lower frequency limits of the decidecade band. For both $L_{p,f}$ and $L_{p,ddec}$, the median and interquartile range of all samples isolated during human review from each turbine operational state are reported. Additionally, the broadband sound pressure level, L_p , was calculated following the same formulation in Equation 2 where f_1 and f_2 are the upper and lower frequency limits, respectively (1 and 100 kHz, described in Section 4.4).

A two-sided Kolmogorov-Smirnov test was utilized as a simple nonparametric test to compare the distributions of decidecade sound pressure levels measured while the turbine was fully operational (100% power) and while it was braked at each hydrophone location. This test is a basic check on whether the sound in each frequency band was significantly different between the two operational states.

Lastly, the weighted cumulative sound exposure level (SEL) was calculated following the U.S. National Marine Fisheries Service (NMFS) technical guidance for assessing the effects of anthropogenic sound on marine mammal hearing (Service 2024). While marine mammals do not inhabit the Kvichak River, this analysis is intended to provide context for the deployment of similar turbines in areas with marine mammals (e.g., tidal channels). The sound exposure level provides an estimate of cumulative auditory impacts when an animal is exposed to an underwater sound for a time, T . NMFS recommends calculating SEL for an exposure period of 24 h (SEL_{24h}) and provides thresholds for SEL_{24h} for five marine mammal hearing groups above which auditory injury is expected. The five hearing groups are as follows: low-frequency cetaceans (LF), high-frequency cetaceans (HF), very high-frequency cetaceans (VHF), phocid pinnipeds (PW), and otariid pinnipeds (OW). NMFS also provides auditory weighting curves for each marine mammal hearing group that weight the sound pressure levels from the source based on the hearing capabilities of marine mammals in that group.

To calculate SEL_{24h} , first we calculated the weighted mean-squared pressure levels, $L_{p,w}(f)$ by applying the auditory weighting curves ($W(f)$) for each of the five marine mammal hearing groups to the median mean-squared pressure levels ($L_p(f)$) recorded at each hydrophone location at each turbine power state:

$$L_{p,w}(f) = L_p(f) + W(f), \quad (3)$$

where $L_p(f)$ and $W(f)$ are both in dB, and $L_p(f)$ has an integration time of 1 s. Because 24 hours of data are not available for each operational state, the median $L_{p,w}$ from each operational state was assumed to be representative of the median sound emitted over 24 hours. $L_{p,w}$ was then adjusted to the weighted 24-hour sound exposure level using:

$$SEL_{24h} = L_{p,w} + 10 \log_{10} T, \quad (4)$$

where T is the exposure duration, in seconds (86400 s). Typically, $L_{p,w}$ in Equation 4 should have an integration time equivalent to T .

4.4 Frequency Limits

As described in Table 3.0, the technical specification states that acoustic measurements should typically be reported between 10 Hz and 100 kHz, but the high frequency limit can be adjusted based on the highest frequency of sound produced by the turbine and the low frequency limit can be adjusted to account for the modal cut-off frequency at the site based on the depth and

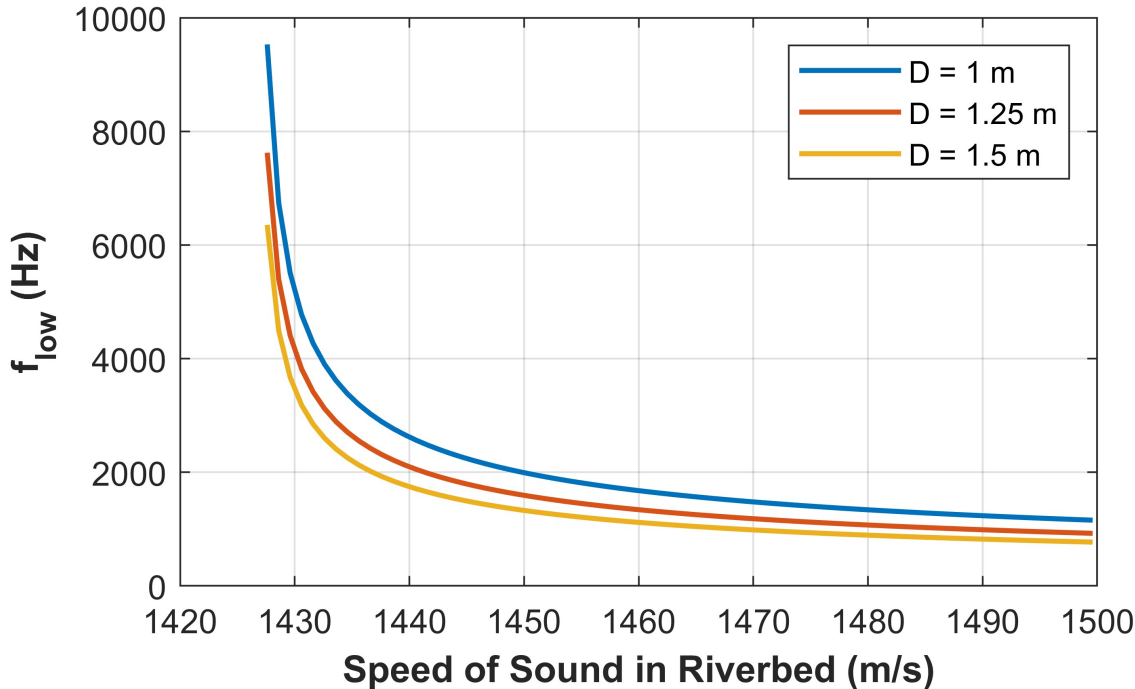


Figure 4. Approximate modal cut-off frequency, calculated using Equation 5, for various values of the speed of sound in the riverbed (c_s) and depth at the hydrophone (D)

sound speed. Because the highest frequency of sound produced by the turbine was not known *a priori*, we use a high frequency limit of 100 kHz. However, the low frequency limit was adjusted based on the modal cut-off frequency due to the shallow water at the location of the hydrophones.

The modal cut-off frequency (f_{low}) can be approximated as:

$$f_{low} = \frac{c}{4D \left(1 - \frac{c^2}{c_s^2}\right)^{\frac{1}{2}}}, \quad (5)$$

where c and c_s are the speed of sound in the water and the seabed, respectively, in m/s , and D is the water depth at the receiver. While we have measurements of c at the test site (Appendix A), we do not have measurements of c_s or the exact water depth at the hydrophone positions (D). Therefore, f_{low} was calculated for a range of reasonable c_s and D values to explore the range of possible modal cutoff frequencies (Figure 4). Only values of c_s greater than c were considered because the speed of sound in coarse-grained sediments, like those found in the Kuchak River, is faster than that of the overlying water (Ballard and Lee 2017). At an estimated hydrophone depth of 1.25 m, f_{low} asymptotically approaches a value around 940 kHz with increasing values of c_s . This trend does not change more than a few hundred Hz for values of D within 0.25 m. We approximate the modal cut-off frequency, and therefore the low frequency limit for freely propagating acoustic signals, to be 1 kHz for calculation of the received broadband sound pressure level at each hydrophone. As described in Section 5.0, this approximation is further supported by the field observations. However, because the relatively close proximity of the hydrophones to the turbine limited the full extent of mode stripping in the propagating signal, sound from the turbine was still observed below 1 kHz. That being said, the received levels in frequencies below 1 kHz were lower than they would have been due to energy loss associated with the modal cutoff. Therefore, we present spectra ($L_{p,f}$ and $L_{p,ddec}$) with a

low frequency limit of 10 Hz and provide a qualitative discussion of turbine sound below 1 kHz.

Hydrophone	Braked	Freewheel	25%	50%	75%	100%
H1	124.0	125.7	125.8	125.8	125.4	125.2
H2	123.6	123.1	122.6	123.0	123.3	123.5
H3	124.3	125.7	126.2	125.6	125.7	125.4
H4	124.5	125.8	126.7	125.9	126.2	125.5

Table 4. Median broadband sound pressure level (L_p) recorded at each hydrophone location, in dB re 1 μ Pa, calculated between $f_1 = 1$ kHz and $f_2 = 100$ kHz.

5.0 Results

Wind speeds remained between a 2 and 3 on the Beaufort Wind Scale on both days of monitoring, with average wind speeds ranging between 2 and 5 m/s. The CTD cast revealed that the river was well mixed, with a mean sound speed of 1426.6 m/s and less than 0.1 m/s of variability with depth. The sound speed profile can be found in Appendix A.

Table 4 shows the median broadband sound pressure level (L_p) recorded at each hydrophone location during each turbine operational state. Figures 5 and 6 show the median and inter-quartile range of the mean-square sound pressure spectral density level and the decidecade sound pressure levels, respectively, for each hydrophone location and each turbine operational state. Figures showing the same data with measurements from each hydrophone for a given power state on the same axes are provided in Appendix B to facilitate comparison between measurement zones.

Figures 5 and 6 reveal several trends in the sound emissions from the turbine. In recordings from all four hydrophone locations, it is evident that, at most frequencies, the turbine produces more sound in lower power generation states and produces the most sound in freewheel. This is likely due to the fact that the turbine has a higher rotation rate during lower power production states, indicating that sound from the turbine is most strongly associated with mechanical noise generated by the rotating turbine components.

At all four hydrophone locations, there is a notable drop in received levels around 1 kHz which we attribute to effects of the modal cut-off frequency (Section 4.4). However, at the hydrophone stations on river right (H2, H3, and H4), sounds from the turbine can still be detected below this low frequency threshold. In fact, at H4, the closest hydrophone to the turbine, tonal peaks are well resolved in frequencies below 1 kHz. Although the flow shields reduced the effect of flow noise, below approximately 100 Hz, the localized effect of non-acoustic pressure fluctuations from turbulence is still evident in baseline data when the turbine was braked at all hydrophone locations. Additional data contamination is observed in data from H1, where a peak in sound pressure levels is observed around 70 Hz both when the turbine is braked and during all turbine operational states. This is attributed to self-noise on the hydrophone lander (e.g., cable flutter). At H1 and H4, sound levels below 100 Hz are elevated above flow noise contamination during all turbine operational states, but little to no signal from the turbine is discernible at these frequencies at H2 and H3. This may be attributed to increased flow speeds in the bypass flow around the turbine during turbine operation.

The characteristics of the low frequency (< 1 kHz) sound associated with turbine operation vary between hydrophone locations and with turbine operational state, suggesting complexity in the propagation of low frequency signals in the shallow riverine environment. During freewheel operation, there is a tone at approximately 100 Hz that is not present when the turbine is generating power. Notably, the 100 kHz tone identified during freewheel operation was only

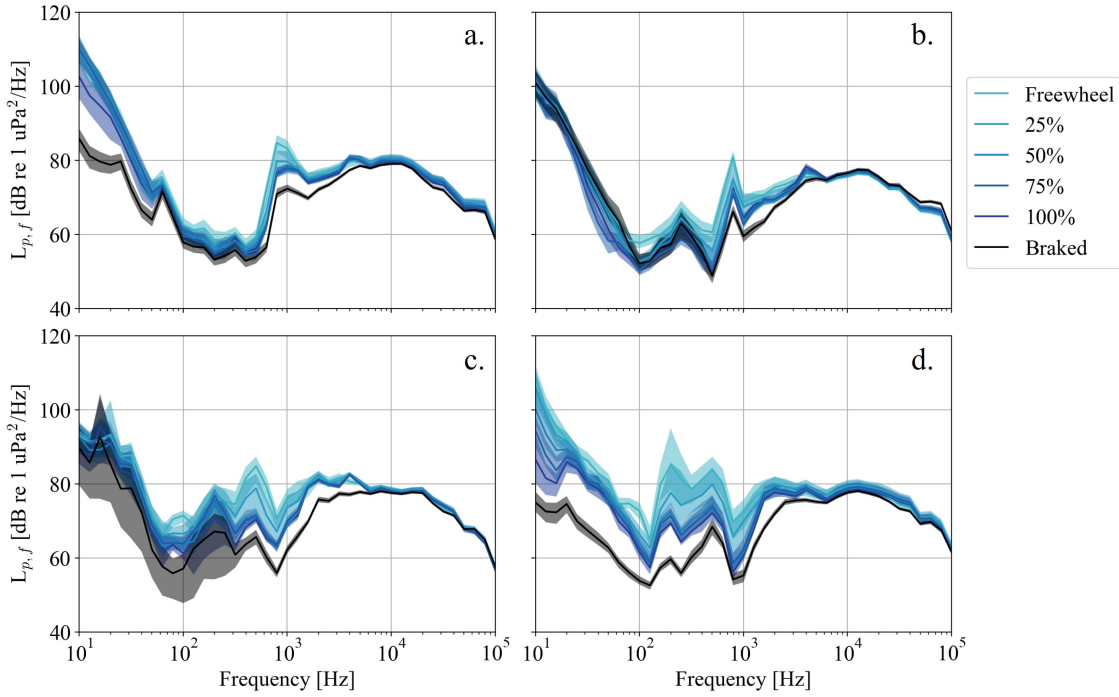


Figure 5. Median decideade sound pressure spectral density levels recorded during each turbine operational state at H1 (a.), H2 (b.), H3 (c.), and H4 (d.). The shaded region indicates the interquartile range.

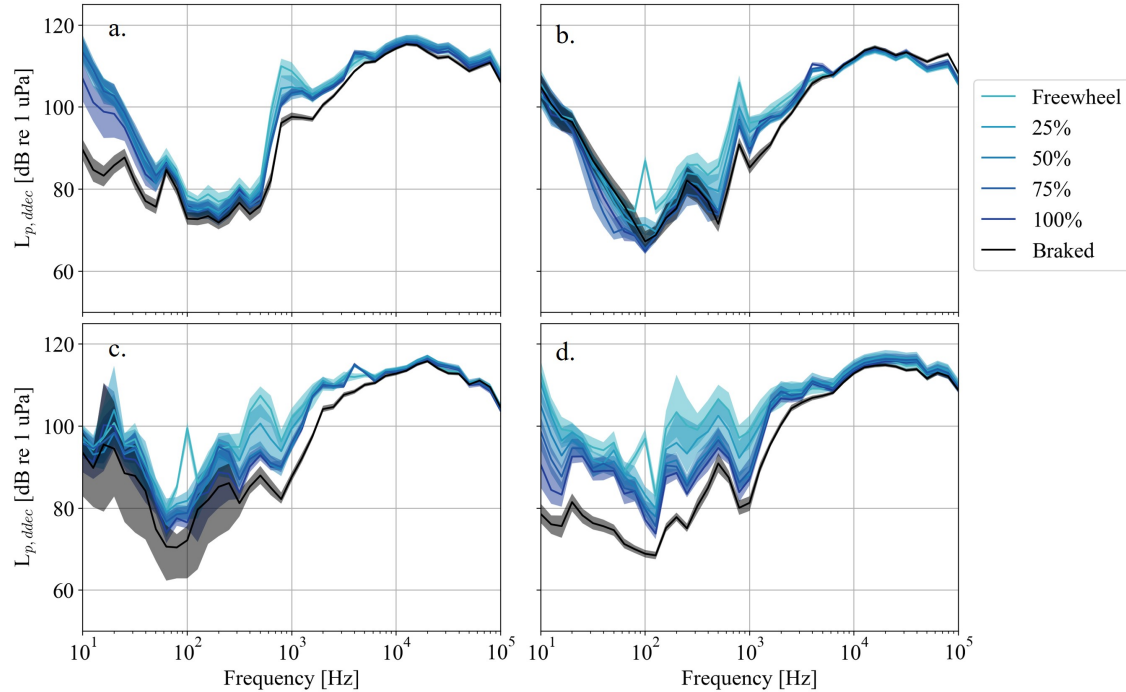


Figure 6. Median mean-squared pressure level recorded during each turbine operational state at H1 (a.), H2 (b.), H3 (c.), and H4 (d.). The shaded region indicates the interquartile range.

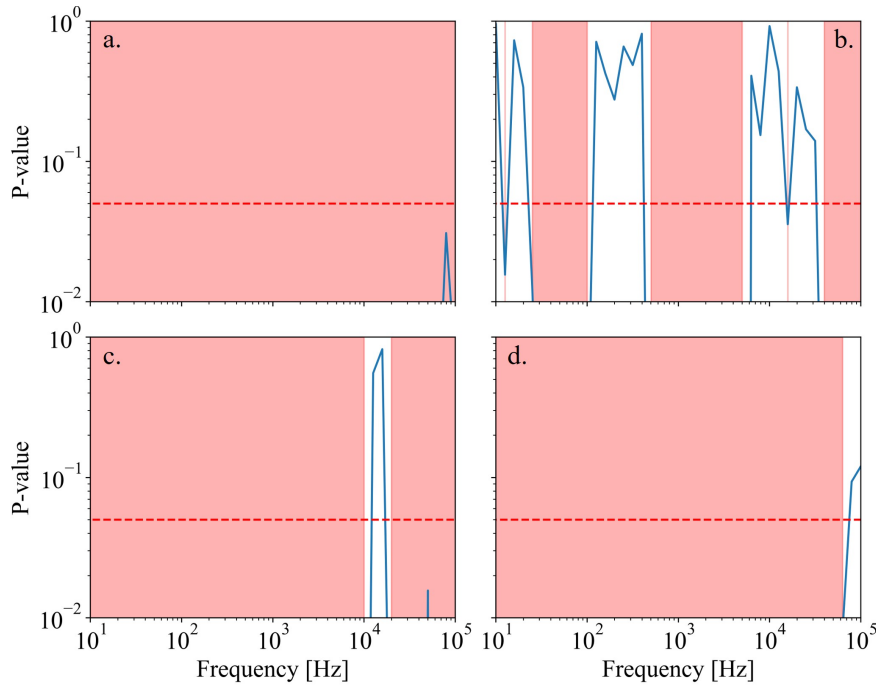


Figure 7. Probability from a two-sided Kolmogorov-Smirnov test comparing decidecade sound pressure levels ($L_{p,ddec}$) measured during 100% power generation and braked operations at sites H1 (a.), H2 (b.), H3 (c.), and H4 (d.). The red dashed line depicts a P-value of 0.05, and the red shaded region covers frequency bands that have a P-value greater than 0.05, meaning the compared distributions most likely do not come from the same distribution.

faintly detectable at H1, but is clear in the signal recorded at H2, which was farther from the turbine. This could be related to differences in the propagation paths from the turbine to the hydrophones with varying bathymetry on either side of the river, or to directionality of the 100 kHz tone (e.g., if the tone originated from a source on the same side of the river as H2).

At frequencies above 1 kHz, similar trends are seen between all hydrophones. Broadband sound levels between 1 and 10 kHz are higher during turbine operation than during baseline (braked) conditions. Additionally, a peak in sound levels between 5 and 6 kHz is observed during turbine power generation in data from all hydrophone locations. This peak is not observed during freewheel operation, so is likely related to the turbine generator. The generator was located on river left (same side of the river as H1), which may explain higher received levels at this location, though we note that baseline sound levels were also higher at this location. Above 10 kHz, sound levels roll off quickly both during turbine operation and during baseline conditions when the turbine was braked, though sound levels are slightly elevated (< 5 dB) between 20 and 50 kHz in recordings from H1, H2, and H4.

Figure 7 shows the results of the two-sided Kolmogorov-Smirnov test comparing the distribution of decidecade sound pressure level measurements measured during turbine operation (100% power generation) and baseline conditions (braked turbine). The results indicate that, at all hydrophones, samples were statistically different ($p\text{-value} < 0.05$) when the turbine was operating. In other words, samples taken while the turbine was operating come from a different distribution than those taken while the turbine was braked. However, this is not true at all frequencies. Notably, at H2, the distributions are not statistically different from approximately 100-700 Hz and 5-20 kHz at H2, and between 10-20 kHz at H3, indicating that

Hearing Group	SEL _{24h} (dB)	NMFS Threshold (dB)
LF	169.7	197
HF	174.9	201
VHF	174.9	181
PW	173.5	195
OW	172.3	199

Table 5. Weighted cumulative 24-hr sound exposure level for each marine mammal hearing group calculated using sound pressure levels measured at H4 during 100% power turbine operation and the NMFS threshold for auditory injury for each hearing group.

the turbine sound was not detected at these frequencies at these locations. This agrees with trends observed in Figure 5; differences in the median and interquartile range of the decidecade level are not visually discernible in these frequency bands.

Weighted cumulative 24-hour sound exposure levels are presented in Table 5 for each marine mammal hearing group using sound pressure levels measured by H4, the hydrophone closest to the turbine (30 m range), during 100% power generation. Sound exposure levels for all turbine power states at all hydrophone locations can be found in Appendix C. Sound exposure levels did not exceed NMFS thresholds for auditory injury for any marine mammal hearing group at any hydrophone location.

6.0 Discussion & Conclusions

In this study, we characterized the acoustic emissions from a riverine turbine using stationary hydrophones deployed on the river banks. The results indicate that, while the turbine does not produce sound at levels predicted to be harmful to marine mammals, it does produce a distinct acoustic signature and sound levels generally increase at lower power states (higher rotation rate). Our results also highlight the complexity of acoustic propagation in rivers; the received acoustic signal from the turbine varied between turbine locations. Further, ambient noise levels when the turbine was braked varied between hydrophone deployment locations, which may be due to a combination of acoustic propagation through the river and differences in local sediment noise.

Given the attenuation of low-frequency sound in the shallow regions of the river where our hydrophone landers were deployed, drifting hydrophones deployed in deeper parts of the river would be likely better suited to measure low frequency sound from the turbine. However, our measurements on the shallow river banks provide a more accurate assessment of the sounds that animals might be exposed to in this portion of the river. Ultimately, acoustic measurements in shallow or constricted environments should be made in the regions of the river where species of interest occur to provide the most accurate estimate of acoustic impacts.

References

Ballard, Megan S., and Kevin M. Lee. 2017. "The Acoustics of Marine Sediments." *Acoustics Today* 13 (3): 11–18.

Cotter, Emma, James McVey, Linnea Weicht, and Joseph Haxel. 2024. "Performance of three hydrophone flow shields in a tidal channel." *JASA Express Letters* 4, no. 1 (January): 016001. <https://doi.org/10.1121/10.0024333>.

Cotter, Emma, Paul Murphy, Christopher Bassett, Benjamin Williamson, and Brian Polagye. 2019. "Acoustic characterization of sensors used for marine environmental monitoring." *Marine Pollution Bulletin* 144:205–215. <https://doi.org/10.1016/j.marpolbul.2019.04.079>.

Forbush, Dominic, Brian Polagye, Jim Thomson, Levi Kilcher, James Donegan, and Jarlath McEntee. 2016. "Performance characterization of a cross-flow hydrokinetic turbine in sheared inflow." *International Journal of Marine Energy* 16:150–161. <https://doi.org/10.1016/j.ijome.2016.06.001>.

Garavelli, L., L.G. Hemery, D.J. Rose, J.M. Farr, and A.E. Copping. 2024. "OES-Environmental 2024 State of the Science Report: Environmental Effects of Marine Renewable Energy Development Around the World." Chap. 3: Marine Renewable Energy: Stressor-Receptor Interactions. <https://doi.org/10.2172/2438589>.

International Electrotechnical Commission. 2019. *Marine Energy = Wave, tidal, and other water current converters - Part 40: Acoustic characterization of marine energy converters*. Technical report IEC TS 62600-40.

Rako-Gospic, Nikolina, and Marta Picciulin. 2019. "Chapter 20 - Underwater Noise: Sources and Effects on Marine Life." In *World Seas: An Environmental Evaluation (Second Edition)*, Second Edition, edited by Charles Sheppard, 367–389. Academic Press. <https://doi.org/10.1016/B978-0-12-805052-1.00023-1>.

Service, National Marine Fisheries. 2024. *Update to: Technical guidance for assessing the effects of anthropogenic sound on marine mammal hearing (Version 3.0): Underwater and In-Air criteria for Onset of Auditory Injury and Temporary Threshold Shifts*. Technical report NOAA Technical Memorandum NMFS-OPR-71. U.S. Dept. Of Commerce, NOAA.

Terrasond. 2015. *Kvichak River RISEC Project Resource Reconnaissance and Physical Characterization, Igiugig, AK*. Technical report. Ocean Renewable Power Company. <https://doi.org/10.15473/1418354>.

Appendix A – Sound Speed Profile

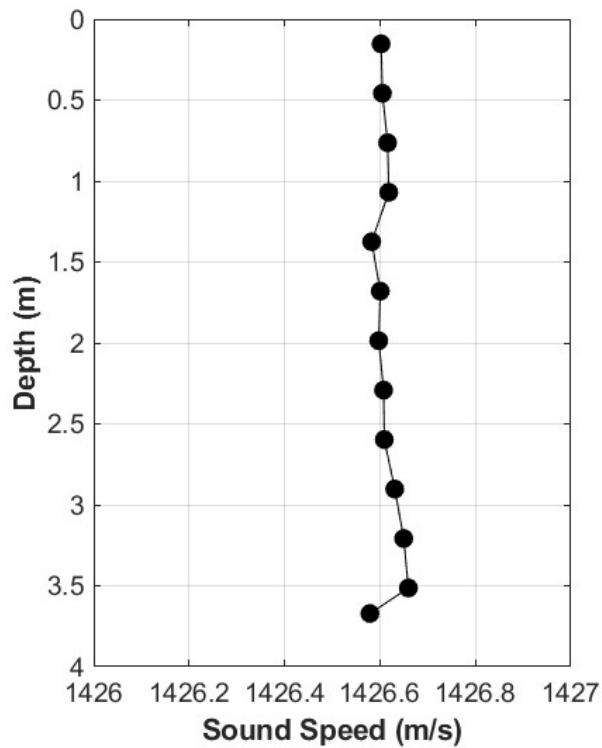


Figure A.1. Sound speed profile measured on 28 May, 2024.

Appendix B – Hydrophone Location Comparison

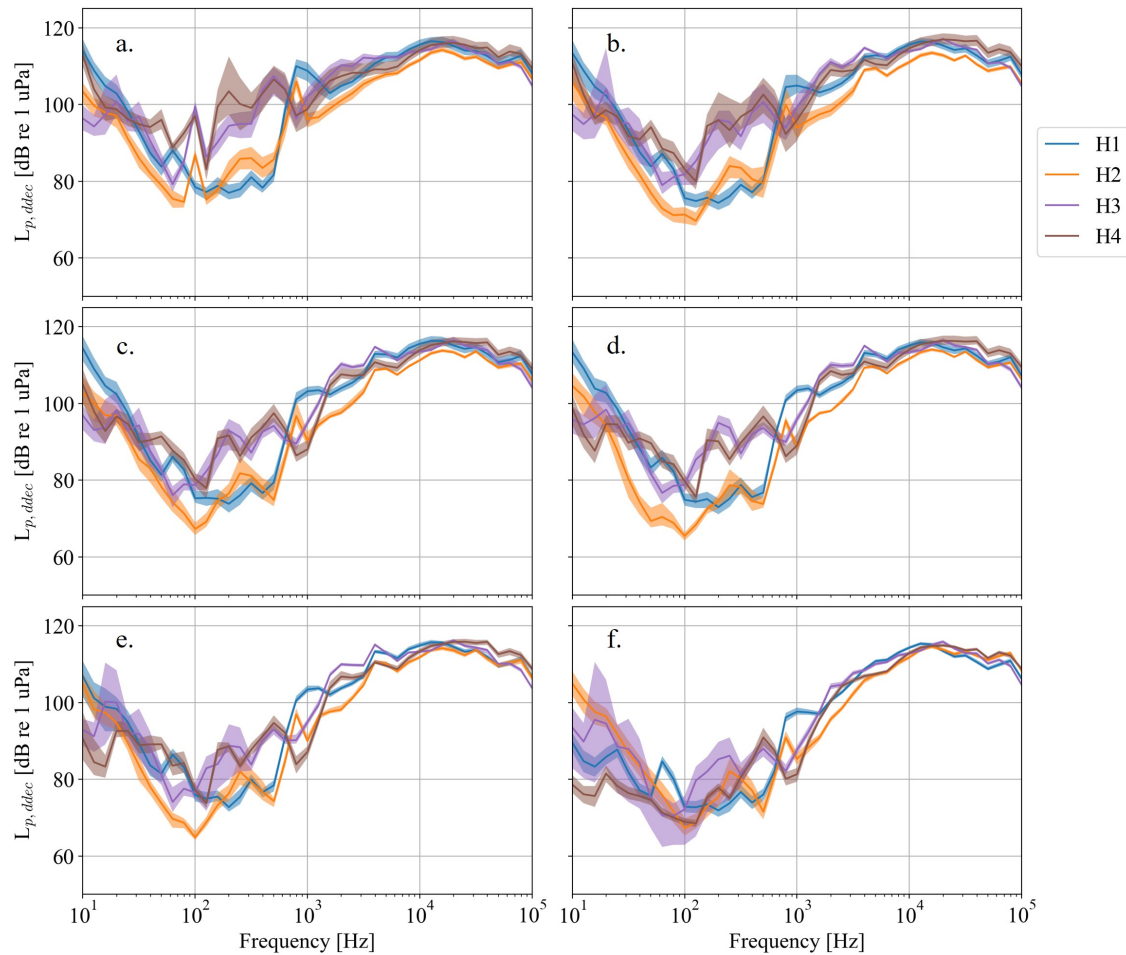


Figure B.2. Median decidecade sound pressure levels recorded at each hydrophone location when the turbine was operated in freewheel (a.), at 25% (b.), 50% (c.), 75% (d.), and 100% power (e.), and when the turbine was braked (f.). The shaded region indicates the interquartile range.

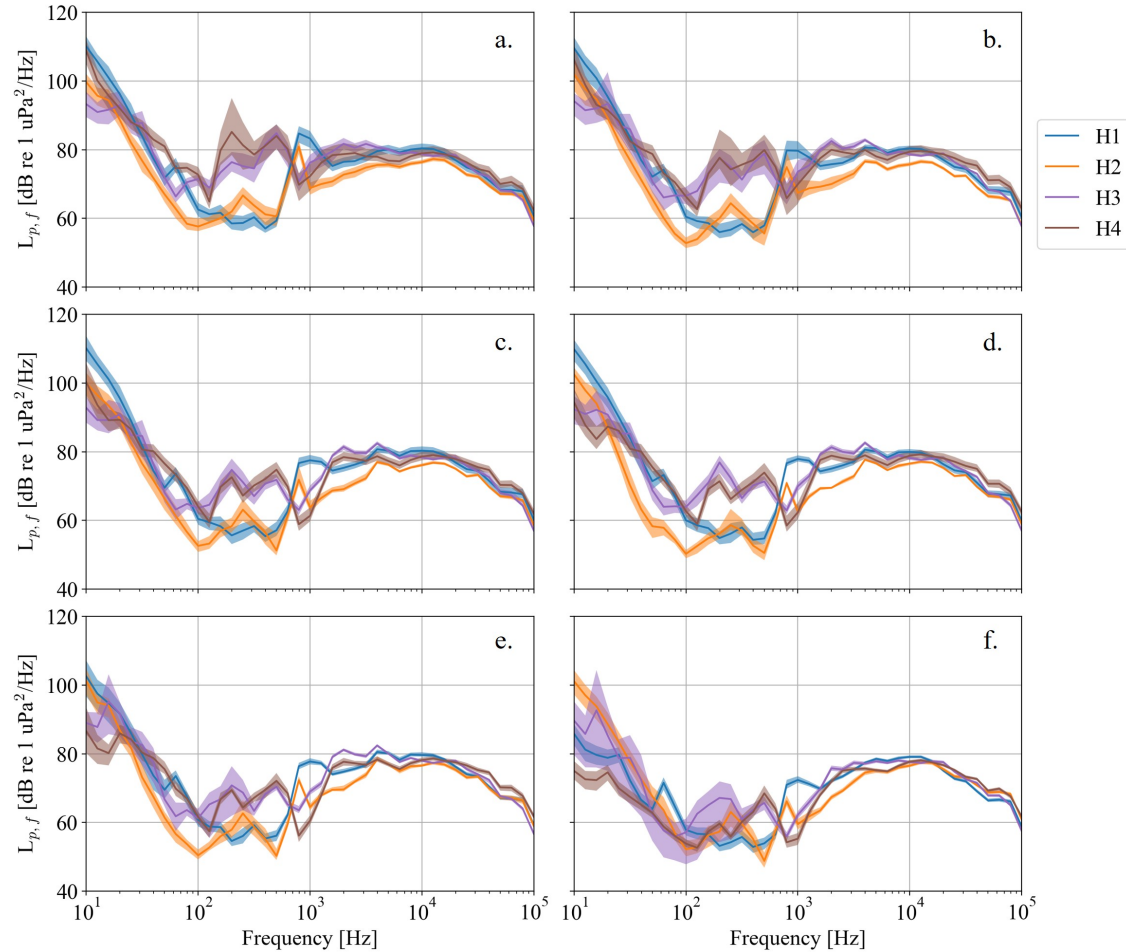


Figure B.3. Median mean-squared pressure spectral density level recorded at each hydrophone location when the turbine was operated in freewheel (a.), at 25% (b.), 50% (c.), 75% (d.), and 100% power (e.), and when the turbine was braked (f.). The shaded region indicates the interquartile range.

Appendix C – Weighted Cumulative Sound Exposure Level

		H1				H2					
		<i>Freewheel</i>	25%	50%	75%	100%	<i>Freewheel</i>	25%	50%	75%	100%
LF	171.1	170.9	170.7	170.5	170.3	167.2	166.9	166.7	167.1	167.4	
HF	174.2	174.4	174.3	174.0	173.7	171.5	171.1	171.4	171.7	171.9	
VHF	173.3	173.4	173.4	173.0	172.7	171.0	170.5	171.0	171.2	171.4	
PW	173.5	173.7	173.5	173.3	173.0	170.5	170.1	170.3	170.7	170.9	
OW	172.7	172.8	172.7	172.5	172.2	169.5	169.1	169.3	169.7	169.9	
		H3				H4					
		<i>Freewheel</i>	25%	50%	75%	100%	<i>Freewheel</i>	25%	50%	75%	100%
LF	171.7	171.3	171.0	171.4	171.8	170.2	170.1	169.8	170.9	169.7	
HF	174.5	174.2	174.4	174.4	174.8	173.4	174.0	174.9	175.2	174.9	
VHF	173.4	173.1	173.5	173.3	173.6	173.1	173.8	174.8	175.0	174.9	
PW	173.9	173.6	173.7	173.9	174.2	172.3	172.8	173.4	174.6	173.5	
OW	172.8	172.5	172.6	172.7	173.1	171.1	171.5	172.2	172.9	172.3	

Table C.1. Cumulative weighted sound exposure level (SEL_{24h}) for each marine mammal hearing group at each hydrophone location and turbine power generation state. SEL_{24h} did not exceed U.S. National Marine Fisheries Service thresholds for auditory injury for any marine mammal hearing group. The five hearing groups are as follows: low-frequency cetaceans (LF), high-frequency cetaceans (HF), very high-frequency cetaceans (VHF), phocid pinnipeds (PW), and otariid pinnipeds (OW).

Pacific Northwest National Laboratory

902 Battelle Boulevard
P.O. Box 999
Richland, WA 99352
1-888-375-PNNL (7675)

www.pnnl.gov